CHEMISTRY
A EUROPEAN JOURNAL

DOI: 10.1002/chem.200901378

Acenaphtho[1,2-*c*]phosphole *P*-Oxide: A Phosphole–Naphthalene π-Conjugated System with High Electron Mobility

Arihiro Saito,[a] Tooru Miyajima,[a] Makoto Nakashima,[a] Tatsuya Fukushima,[b] Hironori Kaji,[b] Yoshihiro Matano,*[a] and Hiroshi Imahori[a, c, d]

Phosphole is known to be a poorly aromatic heterole with a low-lying LUMO due to the effective σ*(P-R)–π*(1,3-diene) hyperconjugation.[1] It is well known that chemical functionalizations at the phosphorus center further reduce the LUMO level considerably. In this regard, phosphole-based π-systems are promising building blocks of π-conjugated materials with both high electron-accepting and electron-transporting abilities.[2] Recently, [*b*]- and [*b*,*d*]-fused phospholes, such as benzo[*b*]phospholes,[2a,g,3a] dibenzo-[*b*,*d*]phospholes,[2f,3b–d] dithieno[*b*,*d*]phospholes,[2d,e,3e–g] and phosphoryl-bridged stilbenes[3h,i] have received growing interest, as they exhibit unique optical and electrochemical properties endowed by the flat, rigid, and elongated π-networks. On the contrary, benzo[*c*]-fused phospholes have been scarcely explored due to their intrinsic instability.[4] We focused on potentially high electron-accepting ability of benzo[*c*]phosphole skeleton[5] and reported the first examples of thermally stable derivatives wherein the bithiophene subunit is [*c*]-fused at the β positions of the phosphole ring.[2b,c] More importantly, the electron mobility of P-oxo derivative **1** (Figure 1) is higher than that of tris(8-hydroxyquinoline)aluminum(III) (Alq_3) at low electric fields. This finding encouraged us to systematically investigate the ring-fusion effects on the electron-accepting and electron-transporting properties of [*c*]-fused phosphole *P*-oxides. In this context, we chose naphthalene as the fused arene framework because its π-system could be easily modulated at peripheral positions. Herein, we report the first comparative study on the optical and electrochemical properties of naphthalene-, acenaphthene-, and acenaphthylene-fused phoshole derivatives. Remarkably, the naphthalene-fused phosphole *P*-oxide (acenaphtho[1,2-*c*]phosphole *P*-oxide) exhibits the highest electron mobility ever reported for phosphole *P*-oxides.

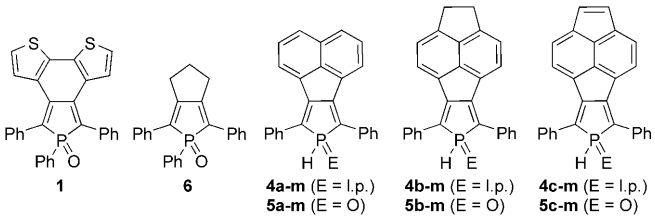

Figure 1. Bithiophene-fused benzo[*c*]phosphole **1**, trimethylene-fused phosphole **6**, and phosphole models **4m** and **5m**. l.p. = lone pair.

Naphthalene-, acenaphthene-, and acenaphthylene-fused phosphole derivatives **3**–**5** were successfully prepared by utilizing a Ti^{II}-mediated cyclization[6] of dialkynylated naphthalene (**2a**),[7] acenaphthene (**2b**), and acenaphthylene (**2c**), respectively, as a key step (Scheme 1). Treatment of gold(I) complexes **3b**,**c** with excess $P(NMe_2)_3$ afforded σ^3-P compounds **4b**,**c**, which were subsequently oxidized by *m*-chloroperbenzoic acid (*m*CPBA) to the corresponding *P*-oxides **5b**,**c**. Compound **5c** was alternatively prepared in 39% yield by dehydrogenation of the bridging ethylene moiety of **5b** with 2,3-dichloro-5,6-dicyanobenzoquinone (DDQ). The *P*-oxides **5a** and **5b** could be directly prepared from **2a** and **2b** in 44 and 48% yield, respectively, without isolating the corresponding σ^3-P intermediates. Compound **4a** was obtained by reduction of **5a** with excess $HSiCl_3$.

[a] A. Saito, T. Miyajima, M. Nakashima, Prof. Dr. Y. Matano, Prof. Dr. H. Imahori
Department of Molecular Engineering
Graduate School of Engineering, Kyoto University
Nishikyo-ku, Kyoto 615-8510 (Japan)
Fax: (+81) 75-383-2571
E-mail: matano@scl.kyoto-u.ac.jp

[b] T. Fukushima, Prof. Dr. H. Kaji
Institute for Chemical Research, Kyoto University
Uji, Kyoto 611-0011 (Japan)

[c] Prof. Dr. H. Imahori
Institute for Integrated Cell-Material Sciences (iCeMS)
Kyoto University, Nishikyo-ku, Kyoto 615-8510 (Japan)

[d] Prof. Dr. H. Imahori
Fukui Institute for Fundamental Chemistry, Kyoto University
Sakyo-ku, Kyoto 606-8103 (Japan)

Supporting information for this article is available on the WWW under http://dx.doi.org/10.1002/chem.200901378.

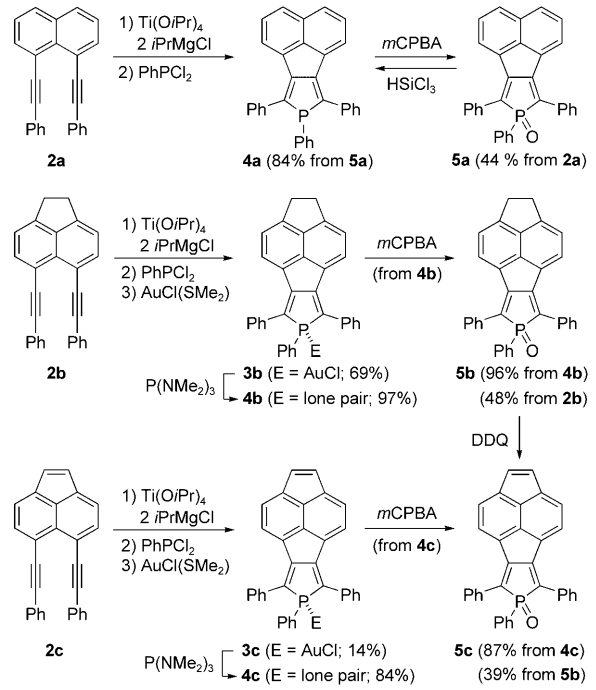

Scheme 1. Synthesis of naphthalene-, acenaphthene-, and acenaphthylene-fused phosphole derivatives **3**–**5**.

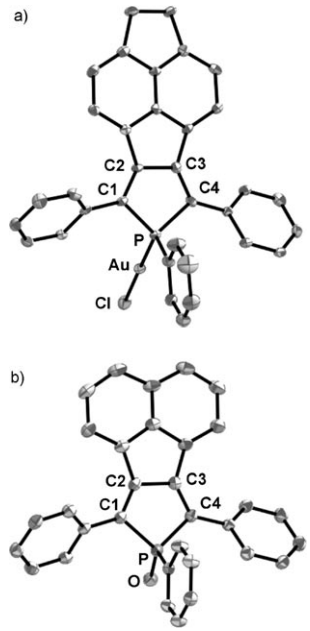

Figure 2. Top views of a) **3b** and b) **5a**. Hydrogen atoms are omitted for clarity. Selected bond length [Å]: **3b**: P–C1 1.798(4); P–C4 1.810(4); P–Au 2.2122(15); Au–Cl 2.2743(15); C1–C2 1.341(5) C2–C3 1.491(5); C3–C4 1.347(5). **5a**: P–C1 1.8174(5); P–C4 1.8184(16); P–O 1.4780(13); C1–C2 1.342(2); C2–C3 1.508(2); C3–C4 1.347(2).

Compounds **3**–**5** were fully characterized by conventional spectroscopic techniques (^{1}H, ^{13}C and ^{31}P NMR, MS, and IR). The ^{31}P peaks of **3**, **4**, and **5** appeared at $\delta = 62.7$–65.7, 40.5–43.9, and 54.5–57.1 ppm, respectively. The structures of **3b** and **5a** were further elucidated by X-ray crystallography (Figure 2).[8] In each compound, the phosphorus center adopts a distorted tetrahedral geometry, and the π-conjugated phosphole and naphthalene rings are nearly on the same plane. On the contrary, the two α-phenyl groups are largely twisted from the phosphole ring with dihedral angels of 37.4–49.0° for **3b** and 40.9–46.7° for **5a**. The C_α–C_β bond lengths [1.341(5)–1.347(5) Å] of the phosphole ring are considerably shorter than the C_β–C_β bond lengths [1.491(5)–1.508(2) Å], reflecting the *cis*-dienic character of the phosphole ring in **3b** and **5a**. The packing structure of **3b** differs from that of **5a** with respect to the mutual orientation of the neighboring phosphole–naphthalene π-systems (Figure S1 in Supporting Information).

To disclose electronic effects of the peripheral and phosphorus substituents on the optical and electrochemical properties of the newly prepared [*c*]-fused phosphole derivatives, we compared the UV/Vis absorption/fluorescence spectra and redox potentials of **4**, **5**, and **6**. The observed data are summarized in Table 1, and the absorption/fluorescence spectra of **4**, **5**, and **6** are depicted in Figure 3 and S2 in the Supporting Information. The absorption and fluorescence maxima (λ_{abs} and λ_{em}) of **5a**–**c** are remarkably red-shifted relative to those of trimethylene-fused reference **6**, indicating that the π-conjugation is effectively extended to the [*c*]-fused π systems. It has been found that the optical properties of the naphthalene- and acenaphthene-fused derivatives (**4a**,**b** and **5a**,**b**) are quite different from those of the acenaphthylene-fused derivatives (**4c** and **5c**). As shown in Figure 3, **5a**,**b** display similar spectral shapes and emit weak

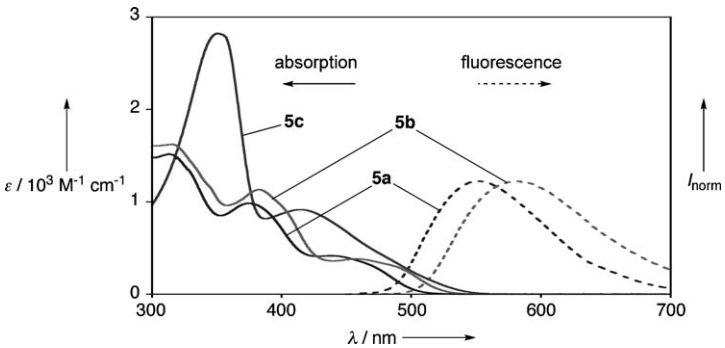

Figure 3. UV/Vis absorption (——) and fluorescence (-----) spectra of **5a**–**c** in CH_2Cl_2.

fluorescence ($\Phi_F = 0.07$–0.08). The lowest transitions of **5a**,**b** are observed at longer wavelength than the corresponding transitions of **4a**,**b**, implying that P-oxidation from **4a**,**b** to **5a**,**b** narrows the HOMO–LUMO gaps of their fused π systems. In sharp contrast, **5c** shows a characteristic intense band at $\lambda_{abs} = 350$ nm, and is non-fluorescent. It should be noted that P-oxidation from **4c** to **5c** makes little impact on the lowest transition, namely the HOMO–LUMO gap of its fused π system (see below).

Table 1. Optical[a] and electrochemical[b] data for **4a–c**, **5a–c**, and **6**.

Compd	λ_{abs}[c] (log ε)	λ_{em}[c] (Φ_F[d])	E_{ox}[e]	E_{red}[e]	ΔE[f]
4a	399 (4.12)	480 (0.38)	+0.64	−2.38	3.02
4b	404 (4.23)	482 (0.23)	+0.52	−2.42	2.94
4c	464 (3.89)	–[g]	+0.74	−1.76	2.50
5a	439 (3.62)	552 (0.08)	+0.94	−1.82	2.76
5b	459 (3.58)	583 (0.07)	+0.77	−1.89	2.66
5c	414 (3.96)	–[g]	+0.98	−1.61	2.59
6	386 (4.15)	491 (0.19)	+1.19	−2.02	3.21

[a] UV/Vis absorption and fluorescence measurements were made in CH_2Cl_2. [b] Redox potentials were determined by DPV in CH_2Cl_2 with 0.1 M $nBu_4N^+PF_6^-$ (Ag/$AgNO_3$). [c] Absorption and emission maxima are given in nm. [d] Fluorescence quantum yield relative to Réau's 3,4-C_4-bridged 1-phenyl-2,5-bis(2-thienyl)phosphole–AuCl Complex (Φ_F = 0.129; ref. [3c]). [e] First oxidation (E_{ox}) and reduction (E_{red}) potentials are given in V versus Fc/Fc^+ couple. [f] $E_{ox}-E_{red}$ (in V). [g] Non-fluorescent.

To gain a deep insight into the electronic structures of the naphthalene-, acenaphthene-, and acenaphthylene-fused phosphole derivatives, we carried out density functional theory (DFT) calculations on model compounds **4x-m** and **5x-m** (**x** = **a**, **b**, **c**) without the phenyl group on the P atom (Figure 1). The C_s symmetric structures of these compounds were optimized at the B3LYP/6-31G* level. As visualized in Figure 4 and S3 in the Supporting Information, the HOMO

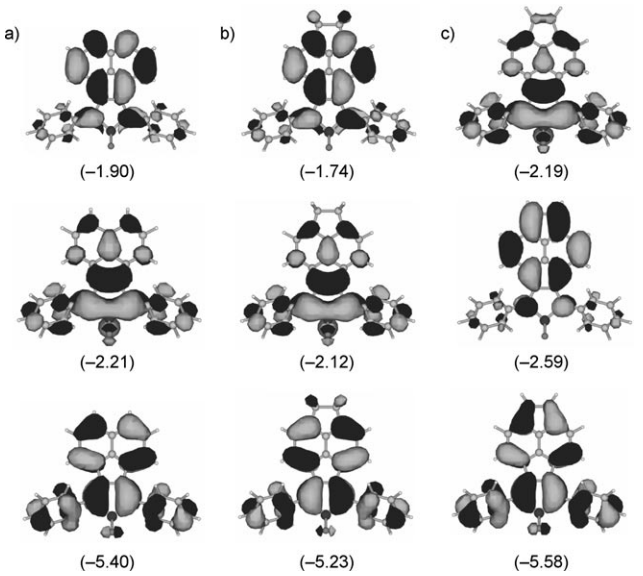

Figure 4. HOMO (lower), LUMO (middle), and LUMO+1 (upper) of a) **5a-m**, b) **5b-m**, and c) **5c-m**. The calculated orbital energies (in eV) are shown in parentheses.

of each model is spread over the entire π-conjugated plane with anti-bonding character between the phosphole and naphthalene rings. On the other hand, the LUMO and LUMO+1 display the character of each subunit. In the case of **5a-m**, the LUMO basically consists of a typical LUMO of phosphole, and the LUMO+1 displays a character of the naphthalene backbone. The LUMO and LUMO+1 of **5b-m** resemble those of **5a-m** with respect to the orbital diagrams and energies. The opposite is noted for **5c-m**; the LUMO has a character of the acenaphthylene subunit, whereas the LUMO+1 possesses a character of phosphole. A similar trend was found for the σ^3-P models (**4a-m**, **4b-m** versus **4c-m**). It is evident that the peripheral functionalizations dramatically alter the characters of LUMO and LUMO+1 of the [*c*]-fused phosphole-naphthalene π-systems.

To reveal the nature of the observed excitations, we also performed time-dependent (TD)-DFT calculations on the models (Table S1 in the Supporting Information). Qualitatively, the theoretically calculated results well explain the experimentally observed absorption spectra. In a series of the σ^3-P derivatives, HOMO–LUMO and HOMO–LUMO+1 transitions of **4a**,**b** are overlapping at around 400–410 nm, whereas the respective transitions of **4c** are observed separately at 464 and 380 (shoulder) nm. In a series of the P-oxo derivatives, HOMO–LUMO and HOMO–LUMO+1 transitions of **5a**,**b** appear separately at 460–490 and 380–400 nm, respectively, whereas those of **5c** are overlapping at around 410–480 nm. Specifically, the P-oxidation considerably stabilizes the phosphole-based π* orbitals (ΔE_{LUMO} = 0.59 and 0.55 eV for the naphthalene- and acenaphthene-fused derivatives; ΔE_{LUMO+1} = 0.53 eV for the acenaphthylene-fused derivative) as compared to the respective HOMO (ΔE_{HOMO} = 0.20–0.21 eV), which results in large red-shifts of the HOMO–LUMO transitions for the naphthalene- and acenaphthene-fused derivatives ($\Delta\lambda$ = 63 and 60 nm) and the HOMO–LUMO+1 transition for the acenaphthylene-fused derivative ($\Delta\lambda$ = 49 nm). It should be noted that the P-oxidation from **4c** to **5c** makes a relatively small impact on the transition from the HOMO to the acenaphthylene-based LUMO ($\Delta\lambda$ = 22 nm).

Redox potentials of **4**, **5**, and **6** were measured by cyclic voltammetry (CV) and differential pulse voltammetry (DPV) (Table 1 and Figure S4 in the Supporting Information). It was found that the electrochemical reduction processes of P-oxo derivatives **5a–c** and **6** occurred reversibly. The first reduction potentials (E_{red}) of **5a–c** are more positive than E_{red} of **6**, indicating that the electron-accepting ability of [*c*]-fused phospholes is appreciably improved by the introduction of the naphthalene, acenaphthene, or acenaphthylene subunit. Among **5a–c**, the difference (ΔE) in the first oxidation potential (E_{ox}) and E_{red} decreases in the order: **5a** (2.76 V) > **5b** (2.66 V) > **5c** (2.59 V). In the cases of the naphthalene- and acenaphthene-fused derivatives, P-oxidation (from **4a**,**b** to **5a**,**b**) shifts E_{red} to the positive side more considerably than E_{ox}. As a result, the ΔE values of **5a**,**b** are smaller than those of **4a**,**b**, which is in good accordance with the results obtained from the absorption spectra and DFT calculations (see above). Most importantly, the above electrochemical data suggested that **5a–c** would be possible candidates for the phosphole-based electron-transporting materials in terms of the electric potential and the reversibility of their reduction processes.[9]

With this in mind, we evaluated the thermal stability of **5a–c**. Compounds **5a** and **5b** were found to be stable up to 250 °C, indicating that the thermal stability of the naphtha-

lene- and acenaphthene-fused phosphole *P*-oxides is reasonably high for device fabrication using high-temperature vacuum deposition.[10] By contrast, **5c** decomposed at 155 °C, implying that the acenaphthylene-fusion does not provide sufficient thermal stability.

At the last stage of this study, we examined the electron mobility of vacuum-deposited films of **5a** and **5b** by the time-of-flight (TOF) technique (for experimental details, see the Supporting Information). Figure 5 shows the field dependency of the logarithmic electron mobilities of **5a**, **5b**, and Alq_3.[2c] Both **5a** and **5b** exhibit the positive field dependency of the electron mobility (μ_E), which increases with increasing the electric field (E). It is remarkable that, at any given electric field, the electron mobility of **5a** is about one-order higher than that of Alq_3.[11] The μ_E value of $8\times10^{-5}\,cm^2\,V^{-1}\,s^{-1}$ observed for **5a** (at $E=1.0\times10^6\,V\,cm^{-1}$) is the highest electron mobility ever reported for the phosphole *P*-oxides.[2a,c,12] These results unambiguously exemplify the high potential of acenaphtho[1,2-*c*]phosphole skeleton for use in electron-transporting organic materials.

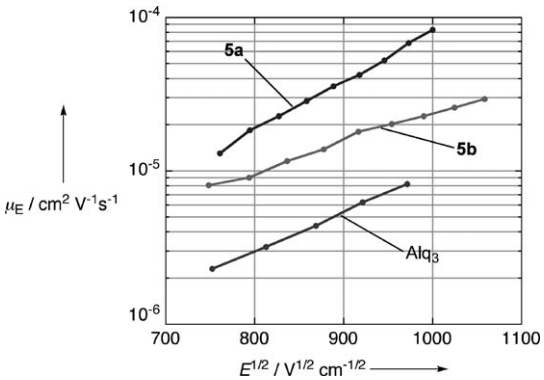

Figure 5. Electron mobilities (μ_E) of **5a**, **5b**, and Alq_3 versus square root of electric field (E).

In summary, we have successfully prepared the first examples of naphthalene-, acenaphthene-, and acenaphthylene-fused phosphole derivatives via Ti^{II}-mediated cyclization of the corresponding dialkynylated arenes. The π-conjugation mode of the arene backbone has a large impact on the optical properties of the [*c*]-fused phosphole derivatives. Among three types of *P*-oxides, the naphthalene- and acenaphthene-fused *P*-oxides exhibit sufficient thermal stability that is prerequisite for the device fabrication using high-temperature vacuum deposition. Notably, the electron mobility of the naphthalene-fused phosphole *P*-oxide is one-order higher than that of Alq_3 at any given electric field. The present results demonstrate that the [*c*]-fusion of the naphthalene ring into the phosphole platform is a highly promising protocol to the development of a new class of phosphole-based π-systems with high electron-transporting ability.

Experimental Section

Typical procedure for the synthesis of 5a (Scheme 1): To a mixture of **2a** (1.92 g, 5.9 mmol), $Ti(OiPr)_4$ (1.7 mL, 5.8 mmol), and Et_2O (175 mL), was added an ether solution of *i*PrMgCl (2.0 M × 5.9 mL, 11.8 mmol) at −50 °C, and the resulting mixture was stirred for 4 h at −40 °C. $PhPCl_2$ (0.80 mL, 5.9 mmol) was then added to the mixture at −40 °C, and the resulting suspension was stirred for 1 h at 0 °C and for an additional 5 h at room temperature. The reaction mixture was then evaporated, and the residue was passed through a short silica gel column (CH_2Cl_2). To the eluent containing the crude product (R_f=0.7) was added *m*CPBA (77 % max, 1.35 g). After stirring for 15 min at room temperature, the reaction mixture was evaporated under reduced pressure. The residue was subjected to silica-gel column chromatography (CH_2Cl_2 → CH_2Cl_2/acetone 30:1). The yellow fraction was collected, evaporated, and precipitated from hexane/CH_2Cl_2 to give **5a** as a yellow solid (1.17 g, 44 %).

Acknowledgements

This work was partially supported by a research grant from The Murata Science Foundation. We thank Dr. Yoshihide Nakao for his helpful suggestions on DFT calculations.

Keywords: electron mobility · electronic structure · fused-ring systems · metallacycles · phospholes

[1] For recent reviews, see: a) F. Mathey, *Angew. Chem.* **2003**, *115*, 1616–1643; *Angew. Chem. Int. Ed.* **2003**, *42*, 1578–1604; b) M. Hissler, P. W. Dyer, R. Réau, *Coord. Chem. Rev.* **2003**, *244*, 1–44; c) L. D. Quin, *Curr. Org. Chem.* **2006**, *10*, 43–78; d) T. Baumgartner, R. Réau, *Chem. Rev.* **2006**, *106*, 4681–4727 (Correction: T. Baumgartner, R. Réau, *Chem. Rev.* **2007**, *107*, 303); e) M. Hissler, C. Lescop, R. Réau, *Pure Appl. Chem.* **2007**, *79*, 201–212; f) M. G. Hobbs, T. Baumgartner, *Eur. J. Inorg. Chem.* **2007**, 3611–3628; g) J. Crassous, R. Réau, *Dalton Trans.* **2008**, 6865–6876; h) Y. Matano, H. Imahori, *Org. Biomol. Chem.* **2009**, *7*, 1258–1271.

[2] For example, see: a) H. Tsuji, K. Sato, L. Ilies, Y. Itoh, Y. Sato, E. Nakamura, *Org. Lett.* **2008**, *10*, 2263–2265; b) T. Miyajima, Y. Matano, H. Imahori, *Eur. J. Org. Chem.* **2008**, 255–259; c) Y. Matano, T. Miyajima, T. Fukushima, H. Kaji, Y. Kimura, H. Imahori, *Chem. Eur. J.* **2008**, *14*, 8102–8115; d) Y. Dienes, M. Eggenstein, T. Kárpáti, T. C. Sutherland, L. Nyulászi, T. Baumgartner, *Chem. Eur. J.* **2008**, *14*, 9878–9889; e) Y. Ren, Y. Dienes, S. Hettel, M. Parvez, B. Hoge, T. Baumgartner, *Organometallics* **2009**, *28*, 734–740; f) K. Geramita, J. McBee, T. D. Tilley, *J. Org. Chem.* **2009**, *74*, 820–829; g) H. Tsuji, K. Sato, Y. Sato, E. Nakamura, *J. Mater. Chem.* **2009**, *19*, 3364–3366.

[3] a) T. Sanji, K. Shiraishi, T. Kashiwabara, M. Tanaka, *Org. Lett.* **2008**, *10*, 2689–2692; b) Y. Makioka, T. Hayashi, M. Tanaka, *Chem. Lett.* **2004**, *33*, 44–45; c) H.-C. Su, O. Fadhel, C.-J. Yang, T.-Y. Cho, C. Fave, M. Hissler, C.-C. Wu, R. Réau, *J. Am. Chem. Soc.* **2006**, *128*, 983–995; d) O. Fadhel, D. Szieberth, V. Deborde, C. Lescop, L. Nyulászi, M. Hissler, R. Réau, *Chem. Eur. J.* **2009**, *15*, 4914–4924; e) T. Baumgartner, T. Neumann, B. Wirges, *Angew. Chem.* **2004**, *116*, 6323–6328; *Angew. Chem. Int. Ed.* **2004**, *43*, 6197–6201; f) T. Baumgartner, W. Bergmans, T. Kárpáti, T. Neumann, M. Nieger, L. Nyulázi, *Chem. Eur. J.* **2005**, *11*, 4687–4699; g) C. Romero-Nieto, S. Merino, J. Rodríguez-López, T. Baumgartner, *Chem. Eur. J.* **2009**, *15*, 4135–4145; h) A. Fukazawa, M. Hara, T. Okamoto, E.-C. Son, C. Xu, K. Tamao, S. Yamaguchi, *Org. Lett.* **2008**, *10*, 913–916; i) A. Fukazawa, H. Yamada, S. Yamaguchi, *Angew. Chem.* **2008**, *120*, 5664–5667; *Angew. Chem. Int. Ed.* **2008**, *47*, 5582–5585.

[4] a) J. M. Holland, D. W. Jones, *J. Chem. Soc. Chem. Commun.* **1970**, 122; b) J. M. Holland, D. W. Jones, *J. Chem. Soc. Perkin Trans. 1* **1973**, 927–931; c) T. H. Chan, K. T. Nwe, *Tetrahedron Lett.* **1973**, *14*, 4815–4818; d) T. H. Chan, K. T. Nwe, *Tetrahedron* **1975**, *31*, 2537–2542; e) A. Schmidpeter, M. Thiele, *Angew. Chem.* **1991**, *103*, 333–335; *Angew. Chem. Int. Ed. Engl.* **1991**, *30*, 308–310; f) A. Decken, F. Bottomley, B. E. Wilkins, E. D. Gill, *Organometallics* **2004**, *23*, 3683–3693.

[5] T. C. Dinadayalane, G. N. Sastry, *J. Chem. Soc. Perkin Trans. 2* **2002**, 1902–1908.

[6] For the syntheses of phospholes via titanacyclopentadienes, see: a) I. Tomita, M. Ueda, *Macromol. Symp.* **2004**, *209*, 217–230; b) Y. Matano, T. Miyajima, T. Nakabuchi, Y. Matsutani, H. Imahori, *J. Org. Chem.* **2006**, *71*, 5792–5795; c) Y. Matano, T. Miyajima, H. Imahori, Y. Kimura, *J. Org. Chem.* **2007**, *72*, 6200–6205; d) T. Sanji, K. Shiraishi, M. Tanaka, *Org. Lett.* **2007**, *9*, 3611–3614; e) Y. Matano, M. Nakashima, H. Imahori, *Angew. Chem.* **2009**, *121*, 4062–4065; *Angew. Chem. Int. Ed.* **2009**, *48*, 4002–4005.

[7] Y.-T. Wu, T. Hayama, K. K. Baldridge, A. Linden, J. S. Siegel, *J. Am. Chem. Soc.* **2006**, *128*, 6870–6884.

[8] **3b**: $C_{34}H_{23}AuClP$, $M_W = 694.91$, triclinic, $0.40 \times 0.20 \times 0.10$ mm, $P\bar{1}$, $a = 10.491(7)$, $b = 10.545(7)$, $c = 12.615(8)$ Å, $\alpha = 94.548(4)$, $\beta = 104.538(11)$, $\gamma = 107.284(4)°$, $V = 1272.0(15)$ Å^3, $Z = 2$, $\rho_{calcd} = 1.814$ g cm^{-3}, $\mu = 59.74$ cm^{-1}, collected 10288, independent 5697, parameters 335, $R_w = 0.0509$, $R = 0.0310$ ($I > 2.00\sigma(I)$), GOF = 1.052. **5a**: $C_{32}H_{21}OP$, $M_W = 452.46$, monoclinic, $0.40 \times 0.20 \times 0.20$ mm, $P2_1$, $a = 11.262(3)$, $b = 8.145(2)$, $c = 12.226(3)$ Å, $\beta = 93.820(4)°$, $V = 1119.1(5)$ Å^3, $Z = 2$, $\rho_{calcd} = 1.343$ g cm^{-3}, $\mu = 1.471$ cm^{-1}, collected 8944, independent 3650, parameters 308, $R_w = 0.0674$, $R = 0.0279$ ($I > 2.00\sigma(I)$), GOF = 1.040. CCDC 729390 (**3b**) and 729389 (**5a**) contain the supplementary crystallographic data for this paper. These data can be obtained free of charge from The Cambridge Crystallographic Data Centre via www.ccdc.cam.ac.uk/data_request/cif.

[9] For each compound, the steady voltammogram was observed after 50 cycles of the potential scan in CV, exhibiting high stability of the *P*-oxides in their electrochemical reduction processes.

[10] Degradation temperatures (Td_{10}, taken at 10% weight loss) of **5a** and **5b** were determined as 343 °C and 371 °C, respectively, by thermogravimetric analysis (TGA) under air.

[11] The electron mobilities of Alq_3 reported by Naka and co-workers are about 2.5 times larger than our experimental values. See: a) S. Naka, H. Okada, H. Onnagawa, T. Tsutsui, *Appl. Phys. Lett.* **2000**, *76*, 197–199; b) S. Naka, H. Okada, H. Onnagawa, Y. Yamaguchi, T. Tsutsui, *Synth. Met.* **2000**, *111–112*, 331–333.

[12] Quite recently, Tsuji and co-workers reported a high electron mobility ($\mu_E = 2 \times 10^{-3}$ cm^2 V^{-1} s^{-1} at $E = 2.5 \times 10^5$ V cm^{-1}) for a benzo[*b*]-phosphole *P*-sulfide. See reference [2g].

Received: May 23, 2009
Published online: August 26, 2009

